International Journal of Engineering Science Technologies
January-February 2026 10(1)
www.ijoest.com

Original Article

PROCESSING OF NI-BASED SUPERALLOYS USING ENERGY-CONCENTRATED CAVITATION WITH HEAVY WATER AND SYNCHROTRON X-RAYS

Toshihiko Yoshimura [1*], **Suguru Ito** [1], **Hiroya Hozumi** [1]
[1] Department of Mechanical Engineering, Sanyo-Onoda City University 1-1-1 Daigaku-dori, Sanyo-Onoda, Yamaguchi 756-0884, Japan

ABSTRACT

An energy-intensive multifunction cavitation process incorporating synchrotron X-rays (PXMEI-MFC) was used to treat the surfaces of the single-crystal Ni-based superalloys SC610 and CMSX-4, employing a mixture of water and heavy water. Similar to data previously obtained from PXMEI-MFC processing using a mixture of acetone and deuterated acetone, the efficiency with which SC610 could be modified was improved compared with that obtained using a laser-irradiated MFC process. However, the water/heavy water system provided a limited processing area compared with the acetone/deuterated acetone system and the alloy surface was not flattened. Although no further oxide film was added, the original oxide layer was not removed and the proportion of the γ' phase was not optimized. In addition, the structure-stabilizing elements Ta, W, and Re did not exhibit significant segregation. Nevertheless, the hardness of the processed region was increased to a greater extent than had been obtained in trials with the acetone/deuterated acetone mixture. Because the degree of processing was improved even with a heavy water concentration of just 1%, it is believed that, during processing of the SC610, heavy water produced higher cavitation collapse pressures and temperatures compared with non-deuterated water. In principle, based on adjusting the balance of various energy inputs, mixtures of heavy water and water should also enable optimization of the γ' phase proportion through self-organization and homogenization of the lattice structures of the γ' and γ phases, similar to mixtures of deuterated acetone and acetone.

Keywords: Synchrotron Radiation, High Energy Multifunction Cavitation, Photoionization, Heavy Water

INTRODUCTION

Hydrogen gas turbines are a vital aspect of achieving a carbon-neutral society. Although current systems operate on the principle of co-firing using 30% hydrogen in natural gas, 100% hydrogen combustion is anticipated in the future. However, turbine blades require further improvements in strength and service life to allow operation at temperatures in excess of 1600 °C. Conventional Ni-based superalloys containing rare metals have been widely used for this purpose but new surface-modification technologies are needed due to concerns regarding cost and structural stability. As shown in Figure 1, the authors previously developed a focused energy multifunction cavitation (MFC) technique combining a water jet, ultrasound, a magnetic field, laser irradiation, and a positron source (PLMEI-MFC) Yoshimura et al. (2023), Yoshimura et al. (2024). When ultrasound is applied to this water jet system, variations in acoustic pressure induce the repeated isothermal expansion and adiabatic compression of air bubbles in the jet to produce high temperatures and pressures within the bubbles Nagata et al. (1992), Suslick et al. (1991), Yeung et al. (1993), Gompf et al. (1997),

*Corresponding Author:
Email address: Toshihiko Yoshimura (yoshimura-t@rs.socu.ac.jp)

Received: 10 November 2025; **Accepted:** 25 December 2025; **Published** 02 February 2026
DOI: 10.29121/IJOEST.v10.i1.2026.733
Page Number: 17-32
Journal Title: International Journal of Engineering Science Technologies
Journal Abbreviation: Int. J. Eng. Sci. Tech
Online ISSN: 2456-8651
Publisher: Granthaalayah Publications and Printers, India
Conflict of Interests: The authors declare that they have no competing interests.
Funding: This research received no specific grant from any funding agency in the public, commercial, or not-for-profit sectors.
Authors' Contributions: Each author made an equal contribution to the conception and design of the study. All authors have reviewed and approved the final version of the manuscript for publication.
Transparency: The authors affirm that this manuscript presents an honest, accurate, and transparent account of the study. All essential aspects have been included, and any deviations from the original study plan have been clearly explained. The writing process strictly adhered to established ethical standards.

Gendanken et al. (2004). The microjets produced during bubble collapse can generate extremes of heat and pressure capable of modifying the surfaces of various material. This process is termed MFC because it can impart advanced surface functionalities Yoshimura et al. (2016), Yoshimura et al. (2018a), Yoshimura et al. (2018b), Yoshimura et al. (2020). This technique was later modified by adding synchrotron X-rays as a photoionization source Rack et al. (2008), Sun et al. (2022), Owen et al. (2016), Fengcheng et al. (2024), resulting in the development of a PXMEI-MFC (Positron X-ray Magnetic Energy Integration – Multifunction Cavitation) system involving synchrotron irradiation Yoshimura et al. (2025-3). This technology generates high temperatures and pressures via the collapse of cavitation bubbles, enabling the strengthening, cleaning, microstructural stabilization, and γ' phase optimization of Ni-based superalloy surfaces. PXMEI-MFC using acetone or deuterated acetone has demonstrated significantly increased bubble temperatures and pressures, leading to the pronounced strengthening of SC610 alloy surfaces together with the removal of oxide films Yoshimura et al. (2025-3).

Heavy water (D_2O) and non-deuterated water (H_2O) exhibit similar physical properties yet differ in vapor pressure, viscosity, and bond energy, and so would be expected to affect the temperatures and pressures associated with cavitation collapse. Theoretically, D_2O should provide stronger adiabatic compression, potentially generating higher temperatures and pressures. In the present study, PXMEI-MFC was applied to the Ni-based superalloys SC610 and CMSX-4 using either water or mixtures of water and heavy water. The goal of this work was to determine whether the strengthening and self-organization effects observed in systems using acetone or deuterated acetone can be reproduced in aqueous systems. Additional aims were to clarify the manner in which variations in the properties of the liquid medium affect cavitation behavior and surface modification and to evaluate the role of photoionization induced by synchrotron radiation.

Figure 1

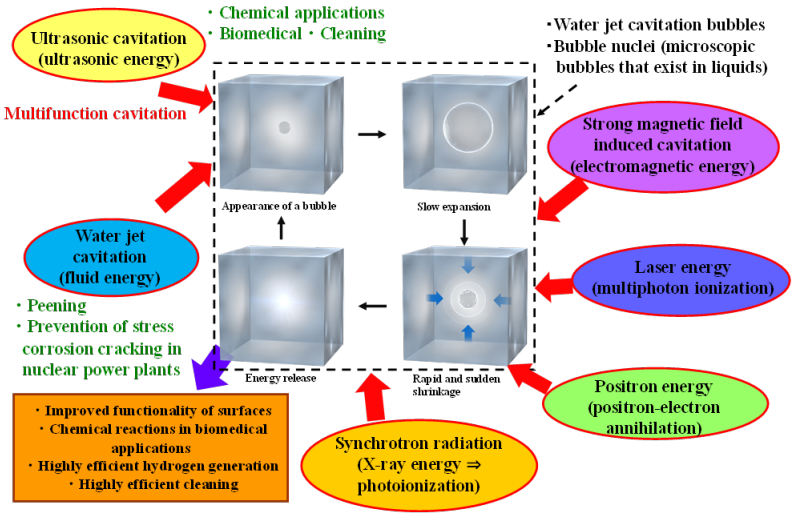

Figure 1 A Summary of Systems for Concentrating Energy in Cavitation Bubbles

MATERIALS AND METHODS

The specimens used in this study were second-generation Ni-based single-crystal superalloys containing Re (SC610-SC and CMSX-4), both of which exhibit high creep strength and excellent oxidation resistance. The chemical compositions of these materials are summarized in Tables 1 and 2. Each specimen had dimensions of ⌀30 mm × 1 mm thickness and was buff-polished sequentially using #80, #220, #500, #800, #1200, and #2000 abrasive papers followed by a final polishing with an oxide suspension. Each specimen was subsequently spot-welded to an electrode and electrolytically polished in a solution of 10% hydrochloric acid and 90% methanol at 3 V DC for 60 s to reveal the crystal structure. PXMEI-MFC processing of the specimens was conducted on the BL09 beamline within the Kyushu Synchrotron Light Research Center.

Figure 2(a) shows the crystal structure of the Ni-based single-crystal superalloys used in this study. These materials each contained an ordered γ' phase and a disordered γ matrix. The γ' phase had an $L1_2$ structure based on a face-centered cubic lattice, as shown in Figure 2(c). The alloys employed in turbine rotor blades experience high temperatures and centrifugal forces during use that can induce structural changes. As shown in Figure 2(b), the γ' and γ phases in such metals align perpendicular to the applied force vector. The resulting creep damage is known as rafting, and elements such as Ta, W, and Re are added to Ni and Al to stabilize the structure and suppress this phenomenon.

The pretreatment of Ni-based superalloy turbine blades typically involves several steps. The surface of each blade is first cleaned with solvents to remove contaminants such as oils, following which the material is polished to eliminate fine defects and remove impurities. The blade is subsequently immersed in a chemical bath to remove surface oxides and contaminants, followed by heat

treatment at a specific temperature to stabilize the internal microstructure. The objective of the work reported herein was to reproduce this complex pretreatment sequence within a single process using the PXMEI-MFC system.

Table 1

Table 1 Chemical Composition of the SC610-SC Alloy used in this Work (mass%)

Cr	Co	Ni	Mo	Hf	Ta	W	Re	Al	Nb
7.4	1.0	Bal.	0.6	0.1	8.8	7.2	1.4	5.0	1.7

Table 2

Table 2 Chemical Composition of the CMSX-4-SC Alloy Used in this work (mass%)

Cr	Co	Ni	Mo	Hf	Ta	W	Re	Al	Ti
6.5	9	Bal.	0.6	0.1	6.5	6	3	5.6	1

Figure 2

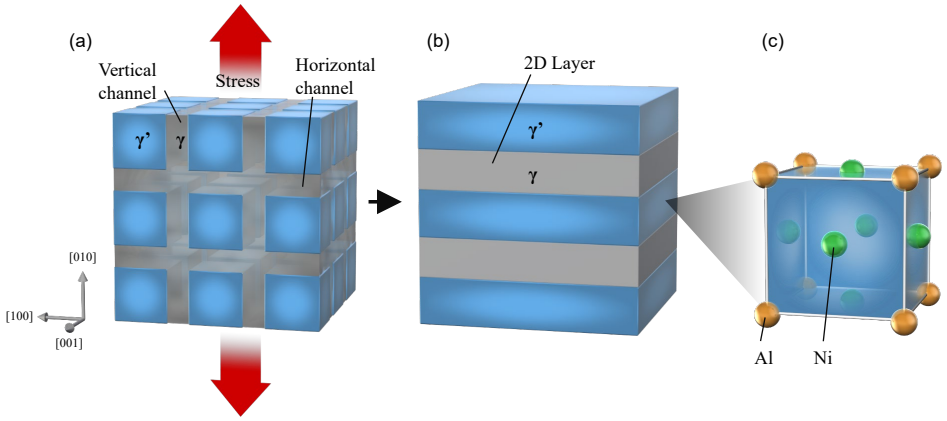

Figure 2 Diagrams Showing an Alloy Specimen (a) before and (b) After Rafting and (c) a Diagram Showing the Crystal Structure of the γ' Phase (that is, the L12 Structure)

It is vital that a Ni-based single-crystal superalloy has optimal proportions of the γ and γ' phases. Specifically, a γ' volume fraction of approximately 70% is considered ideal with regard to maximizing high-temperature performance Caccuri et al. (2017), Yu et al. (2020). This composition enhances both creep strength and structural stability at elevated temperatures. High-temperature casting of these alloys also promotes the formation of a single-crystal structure that improves strength and durability by eliminating grain boundaries. Finally, it is known that controlling the proportion of the γ' phase can maximize creep life. An overly high γ' volume fraction can accelerate the collapse of the rafted structure, potentially reducing creep life. Therefore, it is vital to maintain an appropriate ratio of the two phases.

Ni-based single-crystal superalloys are widely used in components exposed to the highest temperatures in aircraft engines and industrial gas turbines, such as high- and intermediate-pressure turbine blades, vanes, and shrouds. The widespread use of these alloys is attributed to their exceptional mechanical properties at temperatures up to approximately 1150 °C Caccuri et al. (2017), Yu et al. (2020). These superior properties arise from the absence of grain boundaries and the high proportion (approximately 70% in most commercial alloys up to 800 °C) of strengthening γ' precipitates with an $L1_2$ crystal structure coherently embedded within the disordered face-centered cubic γ matrix Caccuri et al. (2017), Yu et al. (2020), Wang et al. (2025), Tan et al. (2025), Wang et al. (2024). Figure 3 presents a diagram of the reaction chamber used in this study [16]. The chamber was filled with water containing 1.0% heavy water that was discharged using a high-pressure pump providing a maximum pressure of 40 MPa and a maximum flow rate of 200 mL/min (L.TEX8731, L. TEX Corporation). The high-pressure mixture of water and heavy water was injected through a 0.2 mm nozzle installed at the center of the tank. The spray pressure was measured using a pressure gauge while the flow rate was monitored using a flowmeter attached to the pump. Although the nozzle of this apparatus is typically made of SUS304 stainless steel, the nozzle employed in the present study was fabricated from the Ni-based superalloy CM186LC to allow the unit to withstand the severe processing environment. The spray pressure and flow rate were 30 MPa and 195 mL/min, respectively. A 22Na positron

source was placed at the top of the tank to irradiate the water surface with positrons and an acrylic lid was installed to prevent water escaping from the chamber. The arrangement of the ultrasonic transducers and neodymium magnets was equivalent to that described in previous reports [1,2]. A mixture of non-deuterated water and heavy water was injected onto SC610 specimens having a columnar-crystal morphology. As cavitation bubbles generated at the nozzle collapsed, numerous new bubbles were formed and the specimen was positioned at the location at which the cavitation cloud was most concentrated.

Five ultrasonic transducers each having a frequency of 28 kHz (WSC28ST standard oscillator and WSC28 integrated custom oscillator, Honda Electronics Company) were placed around the cavitation jet to generate longitudinal acoustic pressure waves. At low acoustic pressures, the bubbles underwent isothermal expansion whereas at high acoustic pressures these bubbles rapidly contracted and experienced adiabatic compression. Repetition of this process generated extremely high temperatures inside the bubbles, enabling cavitation-based processing. A total of 78 neodymium magnets was installed, comprising 39 at the top of the chamber and 39 at the base. The top and bottom of the apparatus corresponded to the north and south magnetic poles, respectively, with magnetic field lines running from the lower right to the upper left of the device. During MFC processing, charged bubbles were generated containing H^+, OH^-, D^+, and OD^- ions generated by thermal decomposition of water vapor together with N+ ions penetrating through the bubble walls. These charged bubbles collided with one another perpendicular to the flow direction as they moved through the strong magnetic field in accordance with Fleming's rule. These collisions produced new high-temperature, high-pressure bubbles, thereby enhancing the processing intensity.

In the case of LMEI-MFC processing, laser light having a wavelength of 450 nm and output power of 42.3 mW was imparted to the cavitation cloud to induce multiphoton ionization inside the bubbles, increasing the ion charge states. This irradiation strengthened the Coulomb interactions between bubbles, resulting in more frequent bubble collisions and an increased number of bubbles. However, because previous studies showed that laser irradiation required processing times exceeding 30 min, high energy monochromatic X-rays generated by synchrotron radiation were used instead of laser light in the present work.

Figure 3

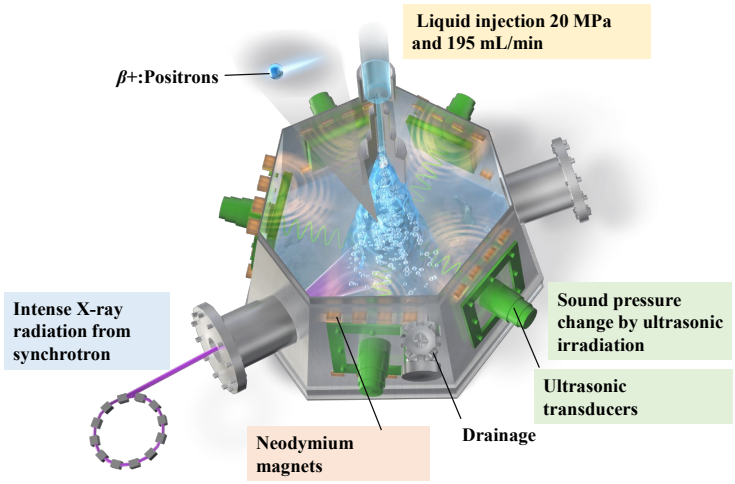

Figure 3 Diagram of the Apparatus used for EI-MFC Processing in a Strong Magnetic Field Together with Synchrotron X-Rays and Positron Excitation

Figure 4 shows the installation of the PXMEI-MFC system on the BL09 beamline at the Kyushu Synchrotron Light Research Center. During these experiments, the BL09 beamline provided a high-flux monochromatic X-ray beam with a uniform wavelength, a beam size of 8 mm (width) × 130 mm (height), an energy of 8 keV, and a photon flux of 5×108 photons/s/mm^2 at 200 mA. To prevent beam loss during transmission through the surrounding air, a rectangular acrylic introduction tube was installed, with its inlet and outlet sealed by 0.05-mm-thick polymer films. This tube was filled with helium. Upon irradiation of the MFC apparatus, positrons underwent partial annihilation through interactions with electrons, producing gamma rays and releasing energy via the reaction $e+ + e- \rightarrow 2\gamma$ (1.02 MeV). In previous studies using this system, a mixture of acetone and deuterated acetone served as the liquid medium. In contrast, the present study employed a mixture of 1% heavy water and 99% water to further increase the temperature and pressure of the bubbles. This mixture was stored in a processing tank and delivered using a high-pressure pump, and the distance between the nozzle and the sample was set to 20 mm. A monochromatic X-ray beam with a height of 8 mm and a width of 130 mm was directed perpendicularly onto the jet at a height of 5 mm above the sample surface.

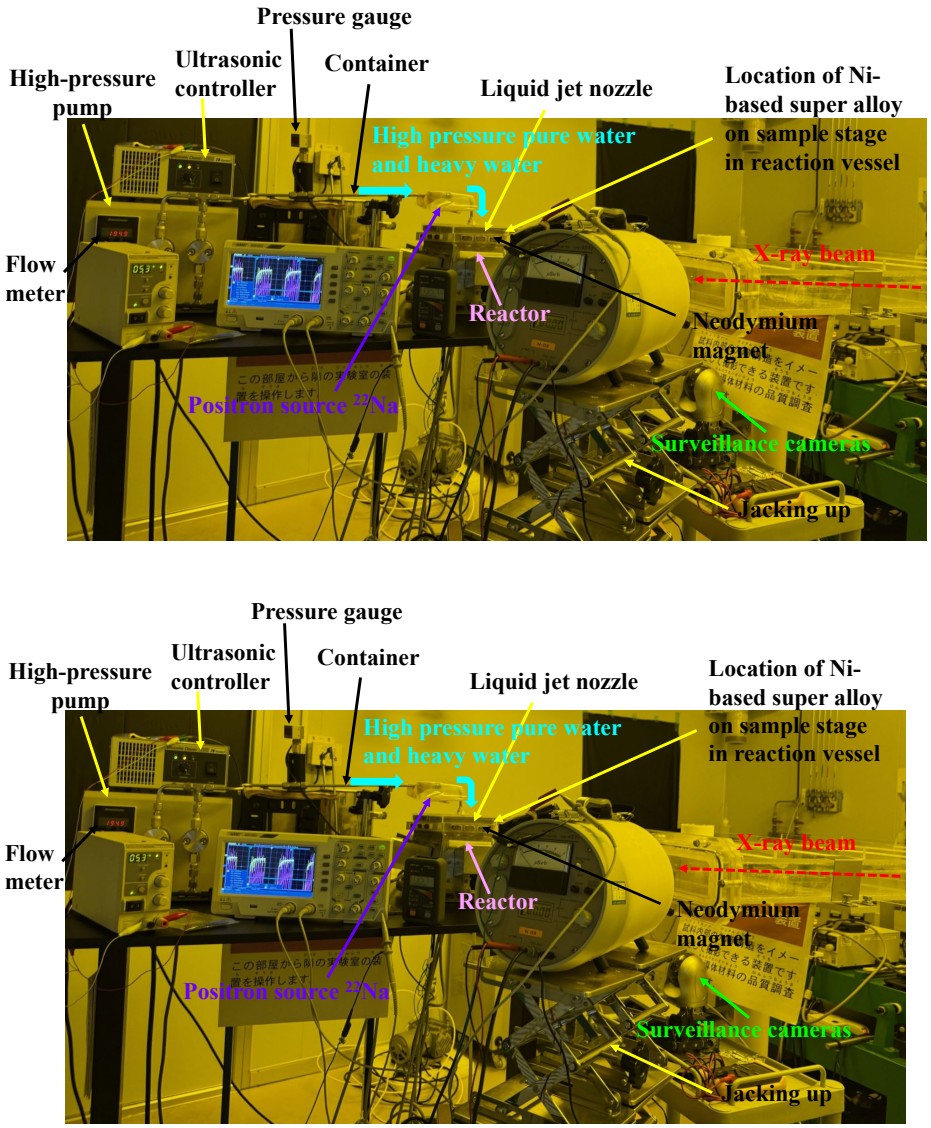

Figure 4 Photographic Images Showing the Installation of the PXMEI-MFC Device on The BL09 Beamline at the Kyushu Synchrotron Light Research Center. (A) the Arrangement of the PXMEI-MFC Experimental Apparatus Prior to X-Ray Irradiation, as Seen Inside the Experimental Hutch, and (B) the PXMEI-MFC Apparatus During X-Ray Irradiation as Seen from Outside the Experimental Hutch

EXPERIMENT RESULTS AND DISCUSSION

Figures 5 and Figure 6 provide scanning electron microscopy (SEM) images of the central surface regions of SC610 specimens processed for 20 min using the PXMEI-MFC system with water and with a mixture of water and heavy water, respectively. When using water as the liquid medium, the lattice structure of the metal was not affected even after the relatively long processing time of 20 min. In contrast, the incorporation of heavy water led to significant disruption of the lattice despite the low heavy water concentration of 1%. It is also apparent from Figure 6 that the γ′ phase was removed to a greater extent than the γ phase.

Prior work using a mixture of acetone and deuterated acetone gave the desired γ′ phase proportion of 70% as a result of self-organization of the alloy, which was not achieved in the present work. In the case of the acetone/deuterated acetone system, the balance of various energies tended to improve the properties of the SC610 and a high-strength surface was formed through self-organization. Figure 7 shows an SEM image of the region surrounding the jet center shown in Figure 6. It can be seen that the lattice structure was disrupted even in this peripheral area and that the γ′ phase was stripped away to a significant depth. Theoretically, it should be possible to induce self-organization of the SC610 surface and to increase the strength of the alloy even when using non-deuterated water. This might require a processing duration that allows diffusion and rearrangement of the alloy atoms to occur near the surface before the γ′ phase is destroyed, to promote self-organization of this phase and give the desired proportion of

approximately 70%. To achieve this, the excess energy imparted to the surface must be suppressed by reducing both the pressure and flow rate. Because SC610 exhibits high strength and a large proportion of the γ′ phase, the application of an excessive impact force leads to the destruction of this phase. Therefore, lowering the water-jet discharge pressure and carefully adjusting the flow rate could prevent damage to this phase while promoting structural ordering.

Figure 5

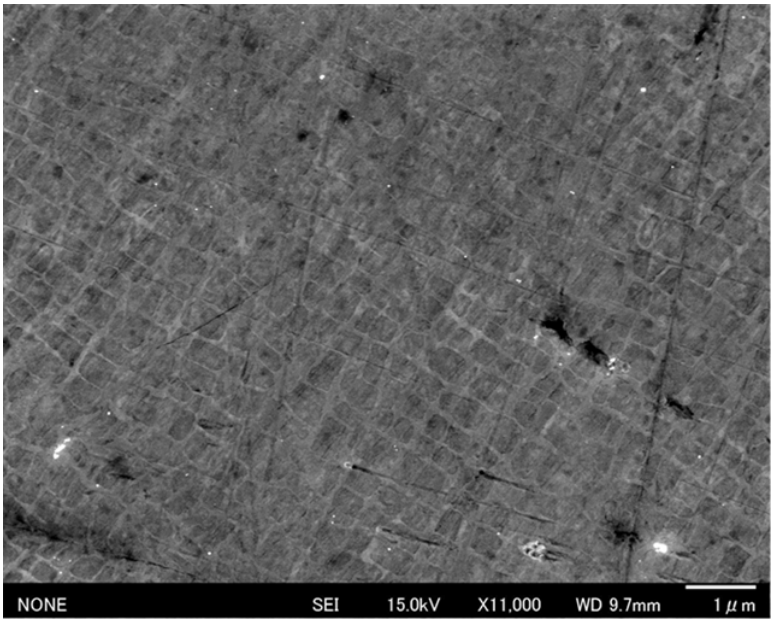

Figure 5 SEM Image of the Central Surface of an SC610 Specimen Processed for 20 Min Using the PXMEI-MFC System with Non-Deuterated Water

Figure 6

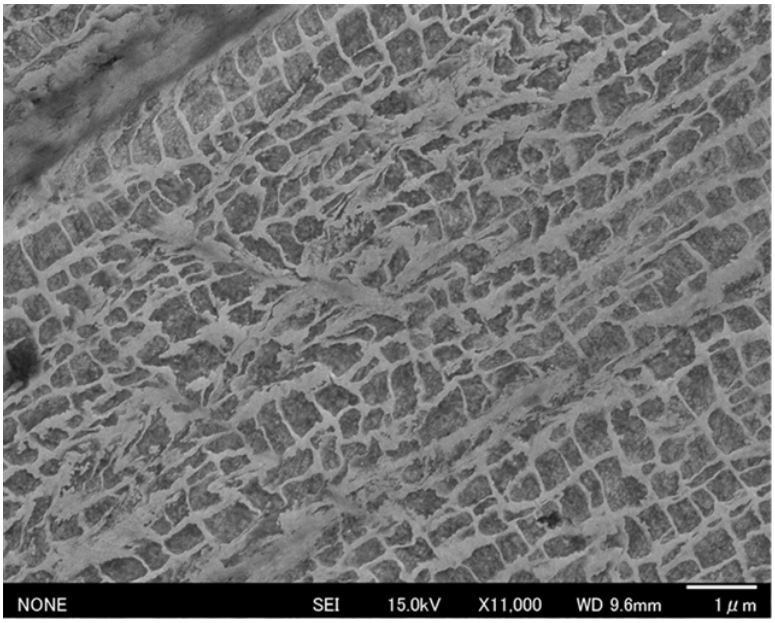

Figure 6 SEM Image of the Central Surface of an SC610 Specimen Processed For 20 Min Using the PXMEI-MFC System with a Mixture of Non-Deuterated and Heavy Water

Figure 7

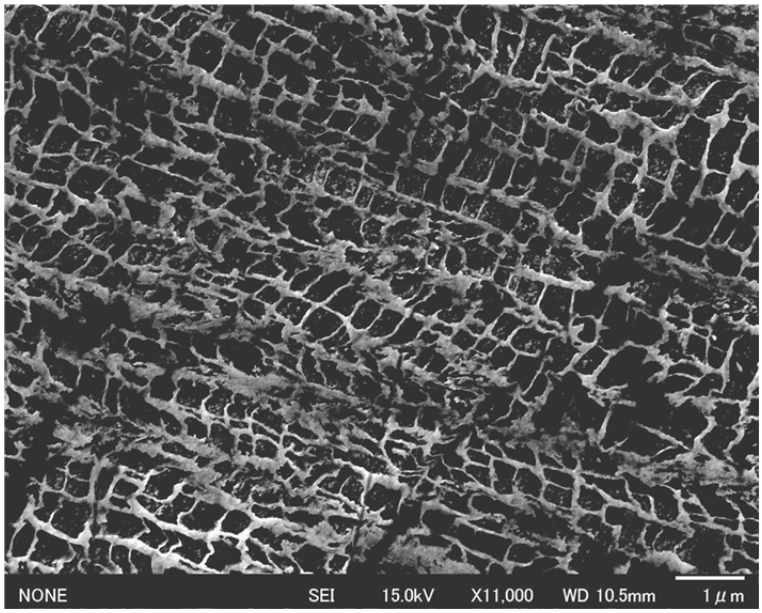

Figure 7 SEM Image of the Surface Around the Processed area of the SC610 Specimen Shown in Figure 6

Figure 8 shows an SEM image of a CMSX-4 specimen prior to processing with the PXMEI-MFC apparatus. It is evident that the γ′ and γ phases were arranged in an orderly manner in this material. Figure 9 presents an SEM image of the region of this sample on which the jet impact was centered after 10 min of processing by PXMEI-MFC using a mixture of non-deuterated and heavy water. Although the γ phase lattice structure exhibits only slight disturbance, etching of the γ′ phase can be observed, similar to the results shown in Figure 6 and Figure 7. Figure 10 shows the binarized version of the SEM image in Figure 9. The γ′phase, indicated in red, accounts for 79% of the image area while the γ phase, indicated in blue, comprises 21% of the total area. In contrast, a mixture of acetone and deuterated acetone previously demonstrated surface strengthening as a result of self-organization to give a γ′ phase proportion of approximately 70% over a wide region. As noted, this is the optimal proportion of this phase with regard to achieving the highest possible strength. On this basis, it is evidently necessary to identify an energy input that provides the appropriate extent of atomic diffusion and reduces the amount of γ′ phase relative to the result shown in Figure 9.

Figure 8

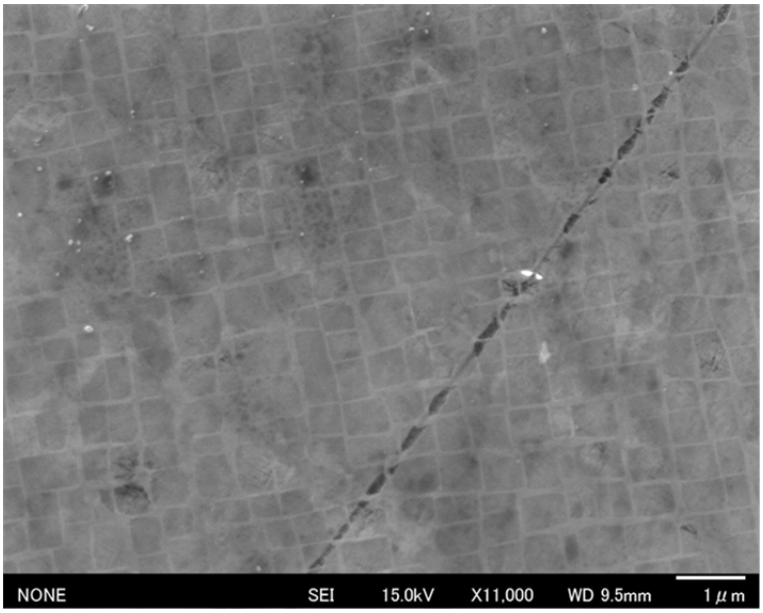

Figure 8 SEM Image Of A CMSX-4 Specimen Prior To Processing By PXMEI-MFC

Figure 9

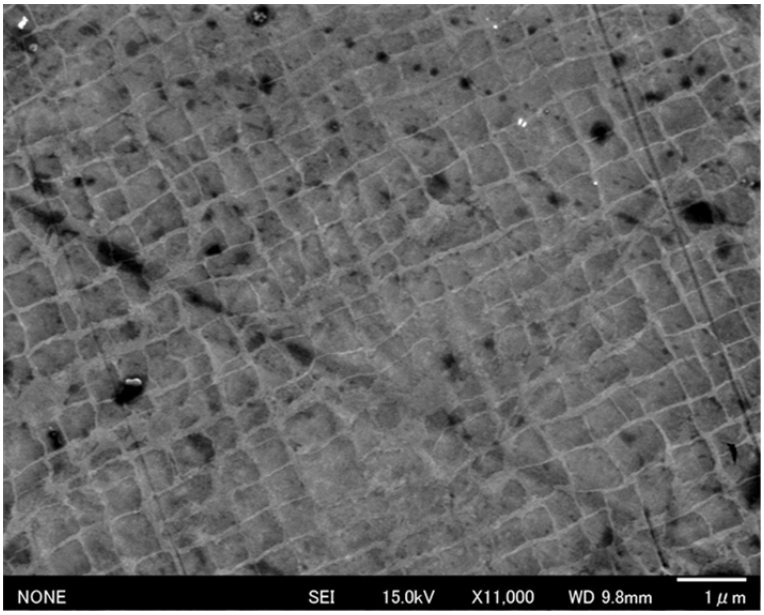

Figure 9 SEM Image of the Center of a CMSX-4 Specimen after 10 min of PXMEI-MFC Processing with a Mixture of Non-Deuterated and Heavy Water

Figure 10

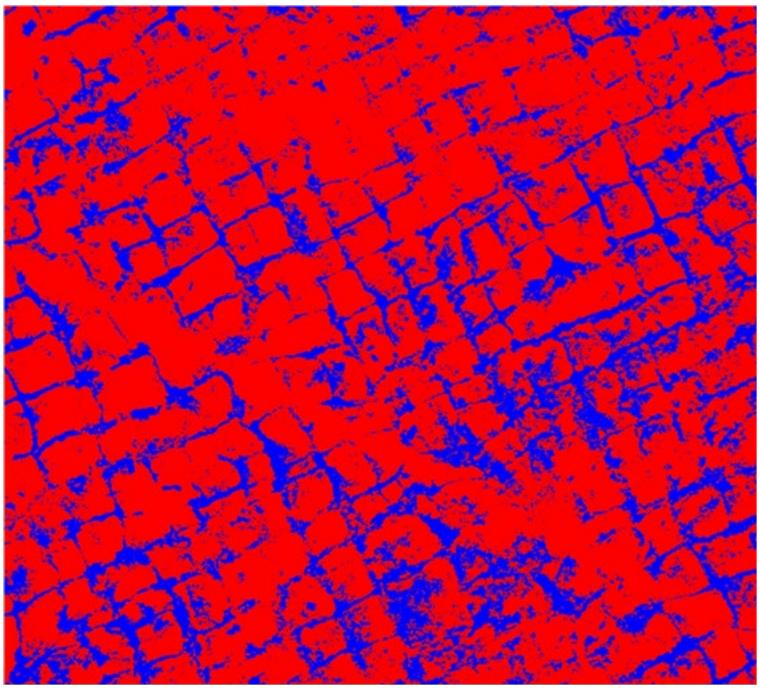

Figure 10 Binarized Version of the SEM Image Shown in Figure 9. The γ' Phase is Shown in red and Comprises 79% of the Specimen while the γ Phase is Shown in Blue and Comprises 21%

Figure 11 provides a laser microscopy image showing the surface of a sample of the Ni-based single-crystal superalloy CM186LC-DS after 10 min of PXMEI-MFC processing using a mixture of acetone and deuterated acetone. A rafting microstructure in which the γ and γ' phases are aligned parallel to one another near the central depression can be observed. It should be noted that rafting does not occur simply as a consequence of a high energy input. Rather, this phenomenon requires a unidirectional stress field together

with sufficient atomic diffusion over an appropriate time scale, and a suitable lattice misfit. The system comprising a mixture of water and heavy water provided high bubble collapse energies but generated a highly disordered and excessive stress field, such that the surface reactions and the dissolution of the alloy were intensified. As a result, rafting did not occur but the γ' phase was damaged and selectively removed. Rafting typically occurs in Ni-based superalloys in response to conditions that promote creep or thermal fatigue. The signs and magnitudes of the γ/γ' phase elastic misfit, the direction of the external stress (whether tensile or compressive), and the temperature/time scale (as required to allow sufficient diffusion) determine whether the γ' phase connects along the stress direction to form a rafted structure, meaning a plate-like arrangement in which γ and γ' phases align parallel to one another. Thus, rafting is not driven by high-energy impacts but by the formation of a directional, quasi-static stress field combined with diffusion-mediated phase rearrangement.

An acetone/deuterated acetone mixture has a lower surface tension than water or heavy water together with a higher vapor pressure. These factors suppress asymmetric bubble deformation during collapse, leading to collapse modes that generate sharp microjets that are less likely to appear in aqueous systems. Consequently, the stresses imparted near the specimen by bubble collapse tend to be more homogeneous and quasi-steady in a time-averaged sense.

The occurrence of rafting in the CM186LC specimen and the formation of a self-organized γ' phase having a proportion of 70% in the SC610 alloy can be attributed to the different energy relaxation pathways arising from alloy-specific characteristics. These characteristics include the initial γ/γ' misfit and the γ' proportion together with the creep strength and deformability of the alloy. In the case of the CM186LC, these conditions favor the formation of a weakly oriented rafted structure, whereas the same conditions promote more uniform self-organization and the formation of an optimal 70% proportion of the γ' phase in the higher-strength SC610 alloy.

The mixture of water and heavy water provided higher bubble collapse energies but the resulting microstructures exhibited lattice disorder, selective removal of the γ' phase, and the absence of a rafted structure. Hence, increasing the energy input did not promote rafting but instead degraded the alloy's lattice structure and enhanced dissolution of the metal. It is possible to suggest a mechanism whereby an excessive energy input prevents rafting. In this mechanism, the stress field becomes highly random and overly intense, thus losing the directionality required for rafting. High-energy aqueous cavitation produces bubble collapses with highly random positions and orientations such that shock waves and microjets impinge on the alloy from multiple directions. As a result, the local stresses are large but lack directionality and also occur in the form of numerous extremely short pulses. This phenomenon resembles a collection of high-speed impacts rather than a creep-like stress field. Under such conditions, the γ' phase does not align directionally and localized shear forces occur along with the formation of defects, lattice decomposition, and alloy dissolution. In the case of the system using a mixture of water and heavy water, interfacial dissolution and chemical reactions will be more important than diffusion-driven ordering. The cavitation in this process will generate radicals that react with dissolved oxygen while localized zones of high temperature and pressure will promote oxidation and dissolution to a greater degree compared with acetone-based systems. Because the γ' phase contains significant amounts of Al, Ti, and Ta in addition to Ni, the chemical properties of this material differ from those of the γ phase, making selective dissolution or degradation possible. The observed lattice disorder and selective removal of the γ' phase indicate that surface/interface destruction and dissolution occurred rather than the microscopic-scale diffusion-driven ordering required for rafting.

Figure 11

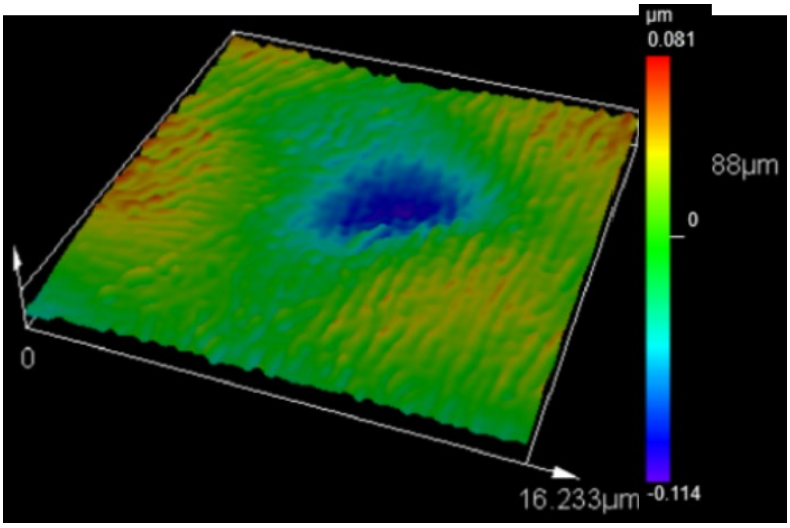

Figure 11 Laser Microscopy Image of the Surface of a NI-Based Superalloy CM186LC-DS Specimen After 10 Min Of PXMEI-MFC Processing Using a Mixture of Acetone and Heavy Acetone

Figure 12 shows a laser microscopy image acquired before 10 min of processing with the PXMEI-MFC apparatus using a mixture of water and heavy water. Similar to the SEM image obtained prior to processing, a lattice structure composed of the γ' and γ phases is apparent. After processing, slight distortions of the lattice structure and localized surface irregularities appear. The arithmetic mean roughness values before processing (Ra: 0.003 µm, Sa: 0.004 µm) were increased to 0.019 µm and 0.007 µm, respectively, after processing Figure 13. However, the surface flattening observed when using a mixture of acetone and heavy acetone was not observed.

Figure 12

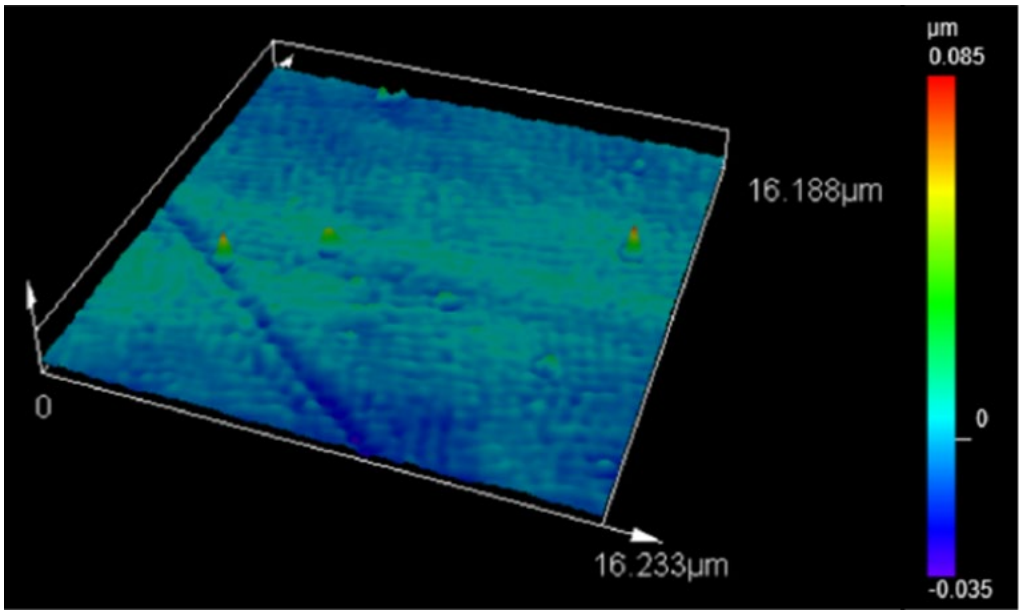

Figure 12 Laser Microscopy Image of a CMSX-4 Specimen Prior to PXMEI-MFC Processing

Figure 13

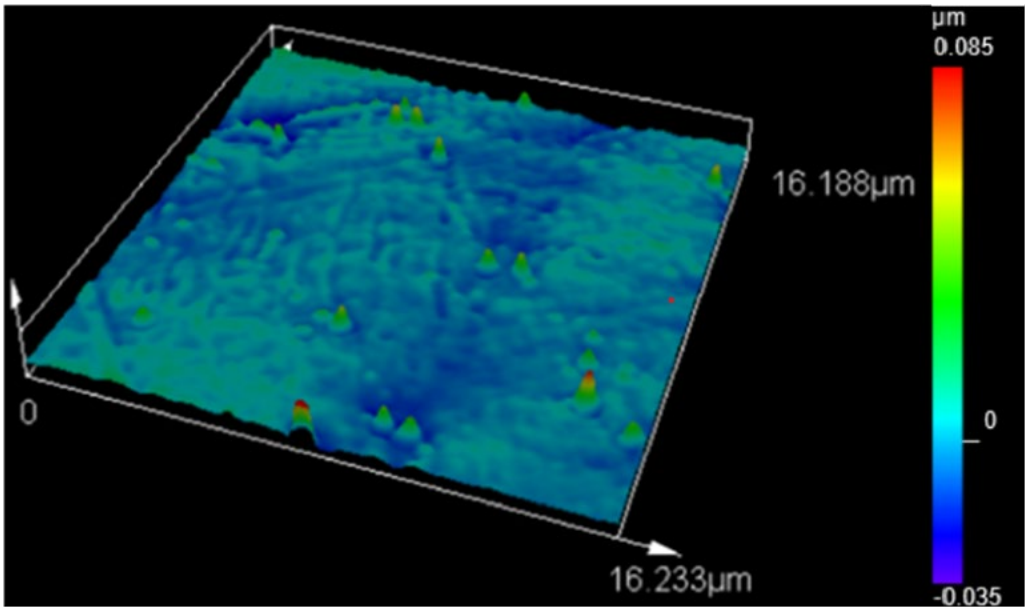

Figure 13 Laser Microscopy Image of the Specimen Shown in Figure 12 After 10 Min Of PXMEI-MFC Processing Using a Mixture of Water and Heavy Water

Figure 14 summarizes the surface roughness values found by laser microscopy at the centers of the processed areas of SC610 specimens treated with the PXMEI-MFC technique under various conditions. A mixture of acetone and heavy acetone decreased the initial arithmetic mean surface roughness, Ra, of 0.017 μm and arithmetic mean height, Sa, of 0.022 μm to 0.009 μm and 0.011 μm, respectively, indicating that the surface was flattened. In contrast, when a mixture of water and heavy water was used, the surface roughness was instead increased after processing under all conditions. In particular, 20 min of processing with water and heavy water increased the initial values of Ra = 0.013 μm and Sa = 0.014 μm to 0.085 μm and 0.072 μm, respectively. These results suggest that microjets generated by cavitation and containing heavy water generated higher impact pressures.

Figure 15 summarizes the surface roughness values determined by laser microscopy around the periphery of the treated areas of SC610 specimens processed under various PXMEI-MFC conditions. Compared with the centers, the overall roughness values for these regions were lower. While the acetone/heavy acetone mixture produced a uniform surface, the water/heavy water combination evidently resulted in a spatial distribution of roughness. Notably, following 20 min of processing with a mixture of water and heavy water, the center region exhibited a sharp increase in Ra from 0.013 μm before processing to 0.085 μm after processing, whereas the peripheral region showed a decrease from Ra = 0.013 μm to Ra = 0.011 μm.

Figure 14

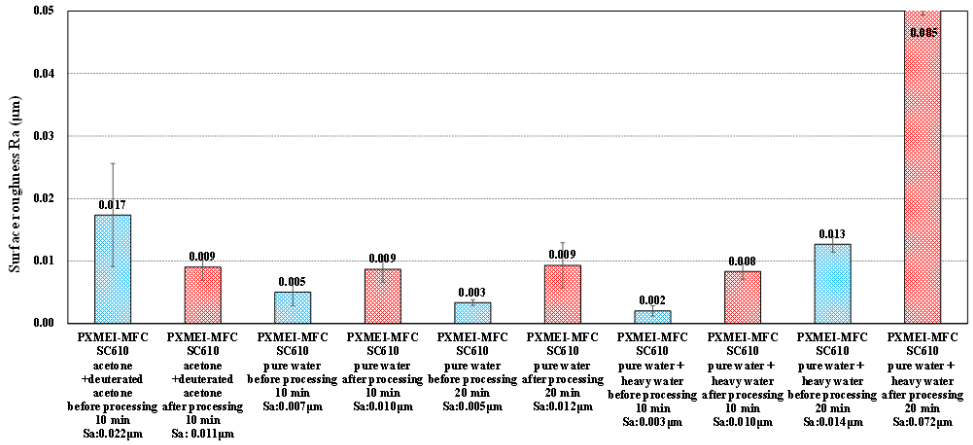

Figure 14 Surface Roughness Values at the Centers of Specimens of the NI-Based Superalloy SC610 After PXMEI-MFC Processing Under Various Conditions as Determined by Laser Microscopy

Figure 15

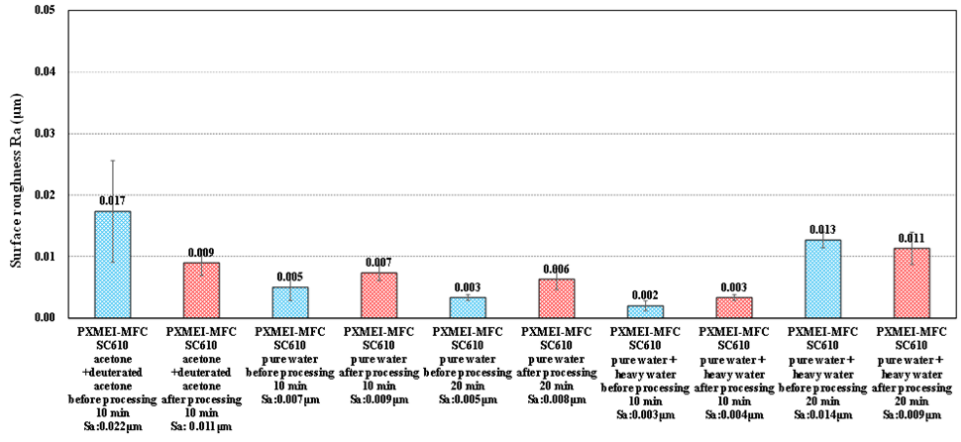

Figure 15 Surface Roughness Values at the Peripheral Areas of Specimens of the NI-based Superalloy SC610 After PXMEI-MFC Processing Under Various Conditions as Determined by Laser Microscopy

Figures 16 and 17 show the surface roughness values at the centers and peripheral regions, respectively, of CMSX-4 samples processed under various PXMEI-MFC conditions. In all cases, the surface roughness was increased after processing. A 20 min treatment using a mixture of water and heavy water provided a maximum value of Ra = 0.113 μm at the center that exceeded the value obtained by LMEI-MFC processing for 30 min. In contrast, within the peripheral region, the roughness decreased from Ra = 0.007 μm before processing to Ra = 0.003 μm after processing, indicating surface flattening. This outcome suggests that the cavitation energy was concentrated at the center of processing, whereas the energy in the peripheral region was at a level more suitable for surface smoothing.

Figure 16

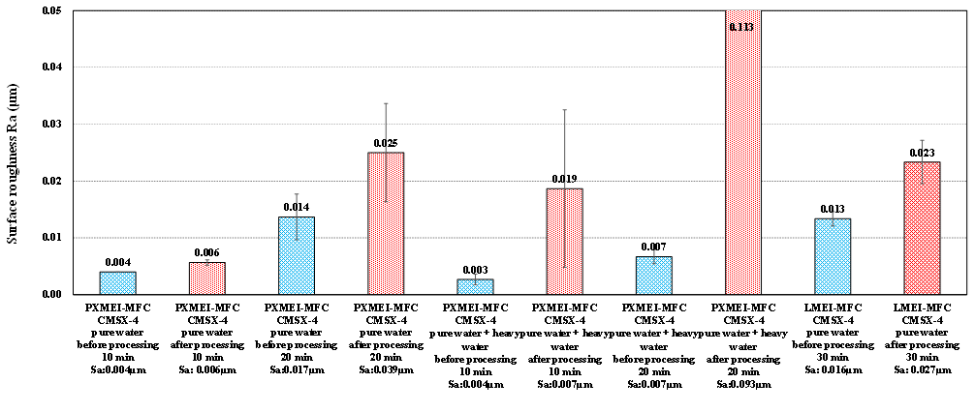

Figure 16 Surface Roughness Values at the Centers of Specimens of the Ni-Based Superalloy CMSX-4 after PXMEI-MFC or LMEI-MFC Processing Under Various Conditions as Determined by Laser Microscopy

Figure 17

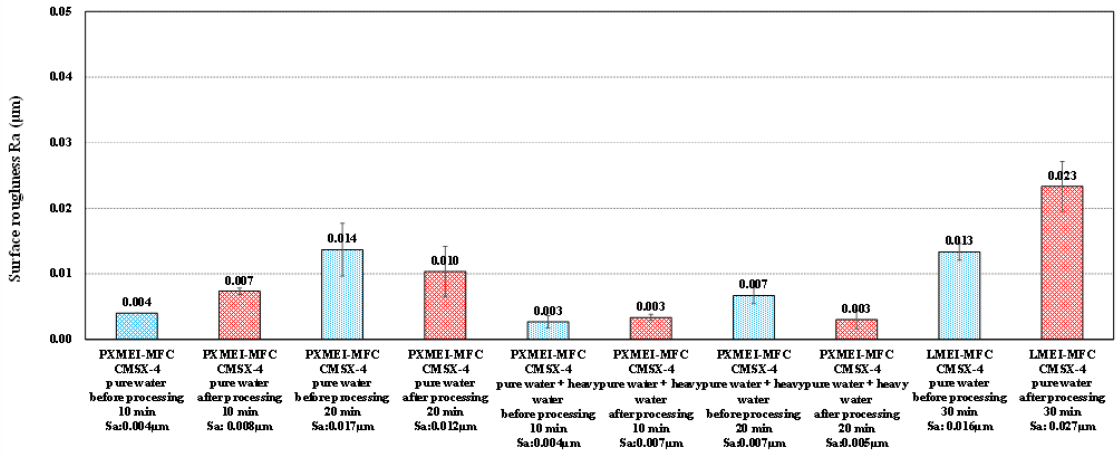

Figure 17 Surface Roughness values at the Peripheral Areas of Specimens of the Ni-Based Superalloy CMSX-4 after PXMEI-MFC or LMEI-MFC Processing Under Various Conditions as Determined by Laser Microscopy

Specimens were characterized by SEM (JEOL Ltd., JSM-7000F) and energy-dispersive X-ray spectroscopy (EDS; Oxford Instruments, X-Max series) before and after processing. When PXMEI-MFC processing was performed using a mixture of acetone and heavy acetone, the microstructure-stabilizing elements Ta, W, and Re were found to diffuse toward the surface and to segregate. In the present experiments using the water/heavy water system, slight surface segregation of Ta was observed in the SC610 specimens at both the jet center and the peripheral regions, while a small extent of W segregation was evident in the CMSX-4 alloy.

Exposure to X-rays can induce both photoionization and radiolysis inside cavitation bubbles, leading to the reduction of oxide films by hydrated electrons (Eaq−) and reducing radicals such as H·. However, the EDS results showed no significant change in the oxygen content of the metal after processing, indicating that the oxide film had not been removed, even though such removal was observed in trials using an acetone/heavy acetone mixture. This finding suggests that the balance of applied energies was insufficient

to induce photoionization or radiolysis. The high water-jet pressure of 30 MPa used in this study produced an extremely high flow velocity, shortening the bubble residence time and the interfacial interaction time. As such, reactive species were likely to disappear before reaching the surface of the metal. Because the radiolysis yield of water or heavy water depends on the absorbed dose and linear energy transfer, reducing the jet pressure while increasing the X-ray intensity could possibly provide better results.

This study originally intended to investigate the compressive residual stresses imparted to alloy surfaces. However, the crystal structures of the Ni-based superalloys could not be confirmed using an X-ray residual stress measurement system. As an alternative, surface hardness data were obtained using a micro-Vickers hardness tester after various cavitation treatments. Because the size of the processed region was limited when using the mixture of water and heavy water, the entire specimen surface was first observed by low-magnification laser microscopy, followed by a high-magnification observation of the processed area. The observation region was then designated using a permanent marker and micro-Vickers hardness measurements were performed within this region. The results for the SC610 and CMSX-4 specimens are summarized in Figure 18 (jet center), Figure 19 (jet periphery), Figure 20 (jet center), and Figure 21 (jet periphery), respectively.

In the case of the SC610 alloy, both 10 and 20 min trials using water resulted in a hardness increase of approximately 80 HV, indicating that varying the processing duration had no significant effect. A 10 min treatment with heavy water also produced an increase of about 80 HV. However, this result may have been influenced by the experimental sequence. In the trial in which the SC610 sample was processed using heavy water for 10 min, 24 L of water and 200 mL of heavy water were added to the tank, whereas only non-deuterated water was present in the reaction chamber. In contrast, the 20 min experiment involving the SC610 alloy was conducted following a 10 min treatment of a CMSX-4 specimen with heavy water, meaning that the reaction chamber already contained a mixture of water and heavy water. As a result, the cavitation generated during the 20 min processing trial involved a greater concentration of heavy water. Treatment of the SC610 with heavy water for 20 min in this manner produced a hardness increase of 130 HV, demonstrating that cavitation in a medium incorporating heavy water at even a low concentration had a greater effect on the alloy. This outcome suggests that the cavitation collapse pressure was increased in the presence of heavy water.

The CMSX-4 specimens exhibited hardness increases ranging from 70 to 90 HV regardless of the processing time (either 10 or 20 min) or the presence of heavy water. Treatment using the LMEI-MFC apparatus involving laser irradiation produced the highest hardness increase of approximately 200 HV. As shown in Figure 16, a Figure 20 min processing trial using the water/heavy water system resulted in significant lattice destruction and a drastic increase in surface roughness. Conversely, the lattice structure composed of γ' and γ phases was preserved after 30 min of LMEI-MFC processing, resulting in higher hardness.

Figure 18

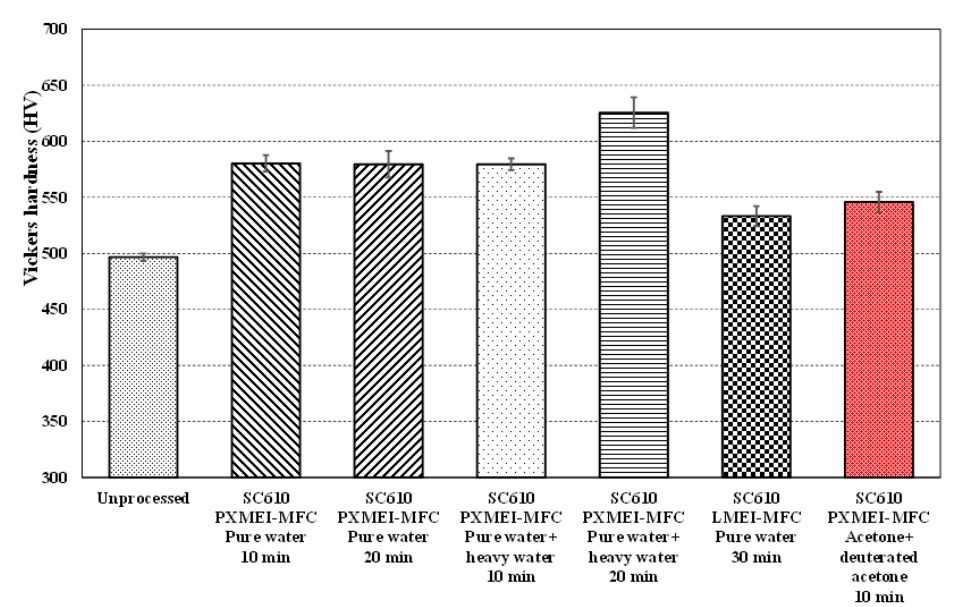

Figure 18 Vickers Hardness Values at The Processing Centers of Specimensof the NI-Based Superalloy SC610 After Processing by PXMEI-MFC Or LMEI-MFC Under Various Conditions

Figure 19

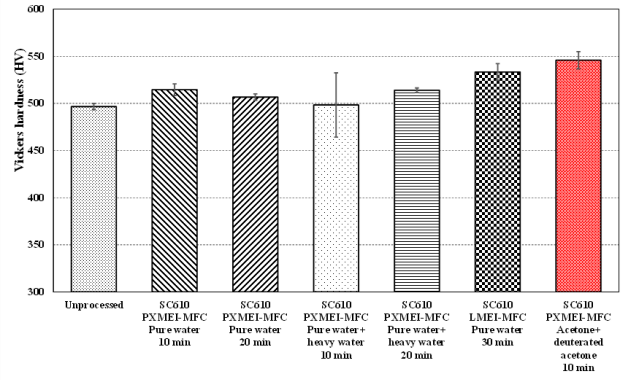

Figure 19 Vickers Hardness Values at the Peripheral areas of Specimens of the NI-Based Superalloy SC610 after Processing by PXMEI-MFC or LMEI-MFC Under Various Conditions

Fiugre 20

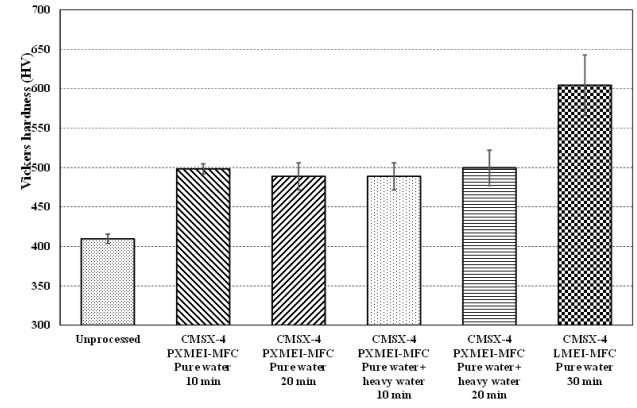

Figure 20 Vickers Hardness Values at the Processing Centers of Specimens of the NI-Based Superalloy CMSX-4 after Processing by PXMEI-MFC or LMEI-MFC Under Various Conditions

Figure 21

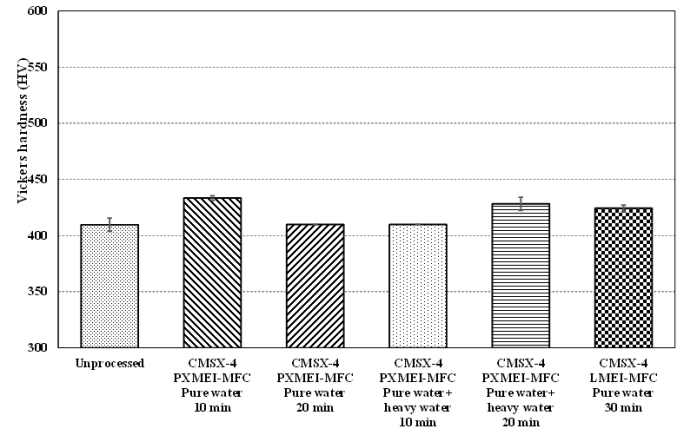

Figure 21 Vickers Hardness Values at the Peripheral Areas of Specimens of the NI-Based Superalloy CMSX-4 After Processing By PXMEI-MFC Or LMEI-MFC Under Various Conditions

CONCLUSIONS

A PXMEI-MFC system incorporating X-ray irradiation from a synchrotron facility was used to process samples of the Ni-based superalloys SC610 and CMSX-4 with a mixture of water and heavy water. In previous work, processing with a mixture of acetone and heavy acetone enabled uniform treatment across the entire specimen. Processing with the present combination of water and heavy water resulted in higher hardness compared with values obtained using the acetone/heavy acetone mixture but over a smaller area. Moreover, no significant surface segregation of Ta, W, or Re, all elements that stabilize the lattice structure, was observed. Interestingly, the addition of even a small proportion of heavy water to the non-deuterated water increased the processing capability of the system. Self-organization of the alloy leading to the formation of a high-strength γ' phase in the ideal proportion of 70% did not occur and the lattice structure of the metal showed both deformation and degradation. Consequently, the single-crystal Ni-based superalloys specimens were not strengthened. To prevent destruction of the γ' phase, it will be necessary to reduce the jet pressure and flow rate to lower the energy input. Because heavy water increases the degree of metal processing to a significant extent at a given jet pressure, the injection pressure must be lowered accordingly.

ACKNOWLEDGMENTS

The authors are grateful to Dr. Kotaro Ishiji of the SAGA Light Source facility for providing invaluable technical assistance and insightful contributions to this research. Dr. Ishiji's expertise and dedication were instrumental in the successful completion of this study.

REFERENCES

Caccuri, V., Cormier, J., and Desmorat, R. (2017). γ′-Rafting Mechanisms under Complex Mechanical Stress state in Ni-Based Single Crystalline Superalloys. Materials & Design,131, 7-497. https://doi.org/10.1016/j.matdes.2017.06.018

Fengcheng, L., Runze, L., Wenjun, L., Mingyuan, X., and Song, Q. (2024). Synchrotron Radiation: A Key Tool for Drug Discovery. Bioorganic & Medicinal Chemistry Letters, 114(1), 29990. https://doi.org/10.1016/j.bmcl.2024.129990

Gendanken, A. (2004). Using sonochemistry for the fabrication of nanomaterials. Ultrason. Sonochem., 11 (2), 47–55. 10.1016/j.ultsonch.2004.01.037

Gompf, B., Gunther, R., Nick, G., Pecha, R., and Eisenmenger, W. (1997). Resolving sonoluminescence pulse width with time-correlated single photon counting. Phys. Rev. Lett., 79, 1405-1408. https://doi.org/10.1103/PhysRevLett.79.1405

Nagata, Y., Watanabe, Y., Fujita, S., Dohmaru, T., Taniguchi, S. (1992). Formation of colloidal silver in water by ultrasonic irradiation. J. Chem. Soc. Chem. Commun., 21, 1620–1622. https://doi.org/10.1039/C39920001620

Owen, R. L., Juanhuix, J., and Fuchs, M. (2016). Current advances in synchrotron radiation instrumentation for MX experiments. Archives of Biochemistry and Biophysics, 602(15), 21-31. https://doi.org/10.1016/j.abb.2016.03.021

Rack, A., Zabler, S., Müller, B. R., Riesemeier, H., Weidemann, G., Lange, A., Goebbels, J., Hentschel, M., and Görner, W. (2008). High resolution synchrotron-based radiography and tomography using hard X-rays at the BAMline (BESSY II). Nuclear Instruments and Methods in Physics Research Section A: Accelerators, Spectrometers, Detectors and Associated Equipment, 586(2), 327-344. https://doi.org/10.1016/j.nima.2007.11.020

Sun, R., Wang, Y., Zhang, J., Deng, T., Yi, Q., Yu, B., Huang, M., Li, G., and Jiang, X. (2022). Synchrotron radiation X-ray imaging with large field of view and high resolution using micro-scanning method. Journal of Synchrotron Radiation, 1241–1250.

Suslick, K. S., Choe, S. B., Cichowlas, A. A., and Grinstaff, M. W. (1991). Sonochemical synthesis of amorphous iron. Nature, 354, 414–416. https://doi.org/10.1038/353414a0

Tan, L., Yang, X. G., D.Q. Shi, W.Q. Huang, Lyu, S. Q., and Fan, Y. S. (2025). Effect of Microstructure Rafting on Deformation Behaviour and Crack Mechanism During High-Temperature Low-Cycle Fatigue of a Ni-Based Single Crystal Superalloy. International Journal of Fatigue, 190(1086199. https://doi.org/10.1016/j.ijfatigue.2024.108619

Wang, P., Wen, Z., Li, M., Lu, G., Cheng, H., He, P., and Yue, Z. (2024). Modified crystal plasticity constitutive model considering tensorial properties of microstructural evolution and creep life prediction model for Ni-based single crystal superalloy with film cooling hole. International Journal of Plasticity, 183(104150). https://doi.org/10.1016/j.ijplas.2024.104150

Wang, R., You, W., Zhang, B., Li, M., Zhao, Y., Liu, H., Chen, G., Mi, D., Hu, D. (2025). Constitutive modeling of creep behavior considering microstructure evolution for directionally solidified nickel-based superalloys. Materials Science and Engineering: A 919, 147499. https://doi.org/10.1016/j.msea.2024.147499

Yeung, S., Hobson, T., Biggs, S., and Grieser, F. (1993). Formation of Gold Sols Using Ultrasound. J. Chem. Soc. Chem. Commun., 4, 378–379. https://doi.org/10.1039/C39930000378

Yoshimura, T., (Inventor). (2020). Assignee: Sanyo-Onoda City public university, Patent no. US, 10(590), 966 B2, Date of Patent, Method for Generating Mechanical and Electrochemical Cavitation, Method for Changing Geometric Shape and Electrochemical Properties of Substance Surface, Method for Peeling off Rare Metal, Mechanical and Electrochemical

Cavitation Generator, and Method for Generating Nuclear Fusion Reaction of Deuterium. International PCT Pub. No.: W02016/136656, Pet Care Trust. No: PCT/JP2016/055016

Yoshimura, T., Maeda, Y., and Ito, S. (2025-3). Development of processing technology for Ni-based superalloys using energy-concentrated cavitation with synchrotron X-rays. Results in Materials, SSRN prerelease. https://papers.ssrn.com/sol3/papers.cfm?abstract_id=5185563

Yoshimura, T., Tanaka, K., and Ijiri, M. (2018b). Nanolevel Surface processing of fine particles by waterjet cavitation and multifunction cavitation to improve the photocatalytic properties of titanium oxide. Intech open access, Open Access Peer-reviewed Chapter 4, Cavitation - Selected Issues, 43-72. http://dx.doi.org/10.5772/intechopen.79530

Yoshimura, T., Tanaka, K., and Yoshinaga, N. (2016). Development of Mechanical-Electrochemical Cavitation Technology. Journal of Jet Flow Eng., 32(1), 10-17, http://id.ndl.go.jp/bib/027265536

Yoshimura, T., Tanaka, K., and Yoshinaga, N. (2018a). Nano-level material processing by multifunction cavitation. Nanoscience & Nanotechnology-Asia, 8(1), 41-54. 10.2174/2210681206666160922164202

Yoshimura, T., Yamamoto, S., and Watanabe, H. (2023). Precise peening of Cr–Mo steel using energy- intensive multifunction cavitation in conjunction with a narrow nozzle and positron irradiation. Results in Materials 20(100463) 1-9. https://doi.org/10.1016/j.rinma.2023.100463

Yoshimura, T., Yamamoto, S., and Watanabe, H. (2024). Precise peening of Ni-Cr-Mo steel by energy-intensive multifunction cavitation in conjunction with positron irradiation. International Journal of Engineering Science Technologies, 8(2), 1–16.

Yu, Z., Wang, X., Yang, F., Yue, Z., James C., and Li, M. (2020). Review of γ' Rafting Behavior inNickel-Based Superalloys: Crystal Plasticity and Phase-Field Simulation. Crystals, 10, (2020)1095. https://doi.org/10.3390/cryst10121095